The 8th European Congress on Computational Methods in Applied Sciences and Engineering
ECCOMAS Congress 2022
5-9 June 2022, Oslo, Norway

# Non-Newtonian Viscous Elongational and Shear Fluid Model based on Optimal Triple Tensor Decomposition

**Markus Rütten**[1,2] **Thomas Schomberg**[2]

[1] German Aerospace Center, Institute of Aerodynamics and Flow Technology,
Bunsenstrasse 10, 37073 Göttingen, Germany, markus.ruetten@dlr.de,
[2]University of Kassel, Institute of Mechanics, Fluid Mechanics Group,
34125 Kassel, Germany

The modeling of the distinct non-Newtonian fluid properties is an essential prerequisite for the computational simulation of associated flow fields. In particular, some non-Newtonian fluids reveal strong diverse viscosity response behaviours to pure elongational and simple shearing flows. Therefore, it is necessary to be able to distinguish between these flow types even in complex flow configuration. Unfortunately flow types are naturally mixed and this distinction becomes quite difficult. Only in a Lagrangian framework the tracking of the Lagrangian fluid element deformation allows an accurate strain related deformation type assignment. However, most CFD approaches prefer the Eulerian framework accepting the loss of the natural flow path alignment of the moving fluid particles. Consequently shear and elongation rates are barely separable without particular assignment methods. In this work a tensor decomposition method from vortex dynamics is discussed which allows to distinguish between these flow types. In vortex dynamics the problem occurred to separate shearing from purely rotational flows because different hydro- and aerodynamic flow phenomena are caused by shear and vortex related flow types. Thereto, various methods were proposed, among others the optimal triple tensor decomposition method which is able to separate vortical from shearing flows but also, after some modification, elongational from shearing flows. This tensor decomposition is now used to calculate elongation and shearing rates as input variables into non-Newtonian fluid models for the calculation of the local elongational and shear viscosity. The application case is a cross slot channel flow often used as reference. In this numerical simulation study the impact of the elongation rate modeling on the contraction flow topology is shown and discussed. It is shown that the modeling of different viscous elongational and shear-thinning affects the resulting flow significantly.

## 1 Introduction

The class of non-Newtonian fluids is very broad and they cover a wide range of fluids in technical applications. Examples of non-Newtonian fluids can be found everywhere in every-day life. Multigrade oils, composite materials, polymers, liquid detergents, paints, printing inks and industrial suspensions all fall within this category as do biological fluids such as blood. In contrast to Newtonian fluids, the properties of non-Newtonian fluids play a significantly more important role in shearing and elongational flows due to their ability to change their viscosity over orders of magnitude in dependence of local shear and elongation rates. In this study focal point is laid on certain non-Newtonian fluids which reveal high sensitivities to the different strain characteristics of shearing and elongation flows leading to distinguishable viscosity changes. In order

to address the impact of different straining motion types on the viscosity it is of fundamental importance to formulate an effective strain type decomposition algorithm capturing the pure features of these fluid deformations. Only then an accurate modeling of the non-Newtonian fluid properties of the considered shearing and elongational fluid flows is possible. Adequate non-Newtonian fluid viscosity modeling together with a suitable CFD grid and a strict numerical simulation strategy are a precondition for reliable simulation results. Non-Newtonian fluids are categorized by their type of constitutive equation. The constitutive equation, which is also called the fluid model, provides essential fluid and, in case, flow dependent information about the quantities which are necessary to close the system of equations in any fluid dynamics problem, i.e. in the momentum equation,

$$\rho \frac{D\vec{v}}{Dt} = -gradp + div\mathbf{T} + \vec{f}\,, \tag{1}$$

whereas incompressible flows are relevant for non-Newtonian flows. In fact, the constitutive equations are used to calculate the stress tensor information which is a correlation between the viscosity and the strain rate, and, in case, other rheological parameters as temperature and pressure. The constitutive equation of Newtonian fluids defines the viscosity as a constant proportionality factor between strain and stress. Therefore, in Newtonian fluid flow case, the viscosity is independent from the flow situation, it is basically a constant. Only a slight dependence on high temperature and pressure changes exists. The constitutive equation of an incompressible Newtonian fluid reads

$$\mathbf{T} = 2\eta\mathbf{D} \tag{2}$$

where $\mathbf{T}$ is the extra-stress tensor, $\mathbf{D}$ represents the rate of deformation tensor and $\eta$ is the viscosity constant which might also be a function of temperature. In non-Newtonian fluid mechanics there is no single rheological constitutive equation which is suitable capturing all fluid material properties in all flow situations. In fact, there are many different possibilities to formulate rheological constitutive equations for the huge variety of these fluids in order to describe their complex, nonlinear viscosity behaviour. For any fluid flow configuration the challenge is to choose an appropriate rheological constitutive equation that encapsulates the actual behaviour of the fluid material in question. More complex fluid specific constitutive equations have to be used to reflect the wide spectrum of sophisticated nonlinear viscoelastic models attempting to capture all of the observed nonlinear viscoelastic phenomena such as elastic recoil, i.e. fluid memory, normal direction shear stress, stress relaxation and elongational viscosity. However, viscoelastic fluid models are not addressed in this work.

Generalized Newtonian fluid models possess the simplest constitutive equations, which are only capable of describing time-independent nonlinear viscous behaviour i.e. when shear-thinning or thickening fluid flow phenomena have to be taken into account. Although the Newtonian fluid cannot describe such shear-thinning or thickening behaviours i.e. of polymer materials, a generalization of equation (2) can be made for the nonlinear shear-dependent viscosity by using the invariants of the rate of deformation tensor:

$$\mathbf{T} = 2\eta(I_D, II_D, III_D)\mathbf{D}\,, \tag{3}$$

in which $\eta(I_D, II_D, III_D)$ is the viscosity function. Models of this type are called Generalized Newtonian fluid (GNF) models. Further simplifications are possible. In incompressible flows, which are relevant in case of non-Newtonian fluids, the first invariant, $I_D$, is zero since it represents the $div\vec{v}$ of the flow field itself. Hence (3) reduces to

$$\mathbf{T} = 2\eta(II_D, III_D)\mathbf{D}\,. \tag{4}$$

In most flow situations, the shear components are dominant, so that the modeling of the viscous behavior is often simplified by taking only the general shear rate to determine the viscosity without treating shear and elongation rates separately. The shear dominance often justifies the assumption to set $III_D$ also to zero. Note that $III_D$ is mostly zero in 2D flows but not the for specific uni-axial extensional flows, latter is an essential presumption that elongational viscosity can reveal thinning or thickening behaviour.

$$\mathbf{T} = 2\eta(II_D)\mathbf{D}\,. \tag{5}$$

This model is often written in terms of the shear rate $\dot{\gamma} = \sqrt{-4II_D}$.
In technical applications the flow configurations and the resulting flow patterns are often complex, hence, there are usually not only shearing components but also stretching components in the local flow. Often in addition to shearing rates, there are comparably significant elongation rates and, hence, elongational viscosity, as Petrie [22] shows, and which was investigated very early on in rheology, see [12] and [20]. It can also be observed that, depending on the flow, the fluid material response to shear or elongation in a very different way, as measurements by [15], [11], [16] have shown. Such measurements are the basis for the principal extensional and shear viscosity curves. In this case it is necessary to introduce separate fluid material models for both shear and elongational flows. That means, if flow simulations are to be carried out with simultaneously occurring shear-thinning and elongational-thickening fluid flow effects, different models have to be used for modeling shear and elongational viscosity. Therefore, in this work focal points are elongational or extensional flows in which the extensional respectively elongational viscosity is one of the important characterizations for flow properties[1]. Since shear flows are most dominant and rheological measurement equipment is especially designed to address them, there have been relatively few elongational viscosity equations incorporated in fluid models in comparison to shear viscosity fluid models. Thus, the formulation of novel elongational viscosity fluid models which are suitable to be applied in polymer processing is a research subject in rheology [28].

## 2 The Problem of Mixed Flow Behaviours

When elongational strain plays a role in the fluid flow application, then the consideration could be made to interpolate between two flow types, whereas the underlying assumption has to be fulfilled that shearing and elongational flows can be categorized as opposite limiting flow cases and an unique assignment of shear and elongation rates can be conducted. Then, simple approaches concentrate on the modeling of the stress information by blending between shear and elongational viscosities applying a kind of weighted blending function:

$$\eta\left(\dot{\gamma},\dot{\epsilon}\right) = \omega \cdot \eta_{\dot{\gamma}}\left(\dot{\gamma}\right) + (1-\omega)\cdot \eta_{\dot{\epsilon}}\left(\dot{\epsilon}\right)\,, \tag{6}$$

Böhme [5], for example, developed the following approach:

$$\eta\left(\dot{\gamma},\dot{\epsilon}\right) = \eta_{\dot{\gamma}}\left(\dot{\gamma}\right) + \sqrt{3\frac{\dot{\epsilon}^2}{\dot{\gamma}^2}}\left[\frac{1}{3}\eta_{\dot{\epsilon}}\left(\dot{\epsilon}\right) - \eta_{\dot{\gamma}}\left(\dot{\gamma}\right)\right]\,, \tag{7}$$

whereas the elongation rate is calculated by

$$\dot{\epsilon} = 6\frac{det\mathbf{D}}{tr(\mathbf{D}^2)}\,, \tag{8}$$

[1] In the related English literature the terms *elongational* and *extensional* are often used optional, which was criticized by [23], who reminded to use exactly defined terms.

which can be reformulated by using the second and the third invariant of the rate of deformation tensor

$$\dot{\epsilon} = \frac{-3III_{\mathbf{D}}}{2II_{\mathbf{D}}} \,. \tag{9}$$

The square of the shear rate can be calculated using $\dot{\gamma}^2 = 2tr(\mathbf{D}^2)$. Such a blending function allows a smooth transition between shear and elongation viscosity whereas the ratio of elongation to shear rates determines the corresponding weight. However, there is the problem that even a calculation of tensor invariants, based on strain rates, can not distinguish correctly between flow types. This is exposed in Table 1, where for different partially mixed flow types the strain rates are expressed in the underlying basic shear and elongation rates.

Table 1: Shear and elongation rates for mixed flow types

| flow type | $\sqrt{-4II_D}$ | $-3\frac{III_D}{2II_D}$ |
|---|---|---|
| uniaxial elongation | $\sqrt{3}\dot{\epsilon}_u$ | $\dot{\epsilon}_u$ |
| equi bi-axial elongation | $2\sqrt{3}\dot{\epsilon}_b$ | $-2\dot{\epsilon}_b$ |
| pure shear | $\dot{\gamma}$ | $0$ |
| uni-axial elongation and shear | $\sqrt{\dot{\gamma}^2 + 3\dot{\epsilon}_u^2}$ | $\dot{\epsilon}_u + \frac{\dot{\gamma}^2\dot{\epsilon}_u}{2\dot{\gamma}^2+6\dot{\epsilon}_u}$ |
| bi-axial elongation and shear | $\sqrt{\dot{\gamma}^2 + 12\dot{\epsilon}_b^2}$ | $-2\dot{\epsilon}_b + \frac{8\dot{\gamma}^2\dot{\epsilon}_b}{2\dot{\gamma}^2+12\dot{\epsilon}_b}$ |

As demonstrated in Table 1, there is no accurate distinction between shear and elongation parts despite their dissimilar physical flow properties and potential impact on the viscosity. Thus, Means [17] and Bobyarchick [4] proposed to derive the ratio of shear and elongation from geometric relations depicted in the Mohr stress circle. Reyn [24] dived deep into local differential equations and classified the flow type by solution properties. Unfortunately, local boundary conditions must be formulated, making it unpractical.In principle those approaches are able to determine the strain directions. However, currently the analytical and computational effort is too high for practical applications, which might change over time with increased computational power.

### 2.1 The Distinction of Different Flow Types

As explained, in flow situations, where shear and elongation flow types are mixed, their different viscosity effects can only be observed when associated strain directions, in which the distinct shear and elongation viscosities are acting, are uniquely determined. Thereto, the intrinsic local coordinate directions shall be adjusted in a way that the diagonal elements of the rate of deformation tensor are only determined by the elongation rates, and the off-diagonal elements are only consisting of shear rates. Then, in principle, the stress tensor could be calculated as follows:

$$\mathbf{T}_{ij} = 2\eta_{\dot{\gamma}}\left(\dot{\gamma}\right)\left(\mathbf{D}_{ij} - \delta_{ij}\mathbf{D}_{ii}\right) + 2\eta_{\dot{\epsilon}}\left(\dot{\epsilon}\right)\delta_{ij}\mathbf{D}_{ii}\,. \tag{10}$$

Unfortunately, in most flow situations the associated basic coordinate system does not exhibit such favourable orientations, so equation (10) cannot be employed immediately, since, in most flow cases, flow direction, coordinate system axes and shear and elongation axes are not aligned. In particular elongation or compression are taking place in direction of the eigenvectors of the material stretching tensor, which can be calculated by applying the Polar decomposition on the absolute deformation tensor. Thus, for further qualification and quantification of deformations

the right Cauchy-Green tensor was analysed. Haller analysed the right Cauchy-Green tensor to identify and classify Lagrangian coherent flow structure assigning it to vortical flows [10], [18]. Nevertheless, even after distinction of the principal deformation axes shear and elongation are not clearly separated. Switching to a Lagrangian perspective delivers a working method to achieve a clear distinction of elongation and compression, shearing and rotation. The advantage is that the undeformed fluid element state is known and can be related to its current deformation. Proper back-projections allow to determine the deformation types. In computational rheology pure Lagrangian solvers are not common, instead mixed Euler-Lagrange solvers are often used [25]. A local Lagrangian coordinate systems is introduced for each grid cell and its deforming motion is observed over time. The Lagrangian information allows to calculate the material stretching tensors and a back propagation on the absolute deformation tensor. However, since additional entrained tensor transport equations have to be solved, the numerical effort is quite high, so this idea was not further investigated so far. Nevertheless, new programming and data management techniques can lead to a revival of Lagrangian simulation tools, so there is a wide field open for further research. In this work a pure Eulerian approach is presented which is based on the idea, that a flow dependend fluid element deformation can be classified by analysing the underlying eigenvectors and their development as Astarita [1] showed. Yao, for example, extended this approach by introducing an objective vorticity to correct rotational deformation effects [29]. Kolář [13] was able to sketch the geometrical relations of fluid element deformation and eigenvector development and to develop a geometrical assignment which finally led to the optimal triple tensor decomposition introduced in the over-next chapter.

### 2.2 Generalized Mixed Strain Tensor Fluid Models

To find the proper principal axes is essential for the accurate shear and elongational viscosity modeling. Thus, the first step of a tensor based fluid model design is to transform the rate of strain tensor into a suitable local coordinate system spanning a new reference frame. The difficulty is to determine the specific transformation tensor, which is discussed in the next chapters. Yet once known, it is applied to the rate of strain tensor $\mathbf{D}$:

$$\tilde{\mathbf{D}} = \mathbf{Q} \cdot \mathbf{D} \cdot \mathbf{Q}^T \,. \tag{11}$$

The second step is to take the components of the local rate of strain tensor $\tilde{\mathbf{D}}$ as input for the calculation of local elongation and shear rates, now in the new references frame. In principle, it it is necessary to transform the rate of strain tensor into two suitable distinct tensors, whereas in the first only diagonal elements appear expressing the elongation and compressing motion, in the second tensor only off-diagonal elements occur manifesting shearing motion. This means the resulting two stress tensors have to be formulated in corresponding shear- and elongation coordinate systems. Then, in principle, between three possibilities to treat the correlation between strain and stress can be chosen:
The first is to use the new tensor information only to determine the distinct shear and elongation rates as input into a weighted viscosity function similar to the approach of equation (7):

$$\eta\left(\dot{\gamma}^*, \dot{\epsilon}^+\right) = \omega \cdot \eta_{\dot{\gamma}}\left(\dot{\gamma}^*\right) + (1-\omega) \cdot \eta_{\dot{\epsilon}}\left(\dot{\epsilon}^+\right) \,. \tag{12}$$

For the calculation of the stress itself the regular GNF, see equation (3), approach with the original rate of strain tensor is used.
The second method is also inspired by the GNF model approach, but here the transformed strain tensor information are also used to calculate the corresponding stress tensors for shear

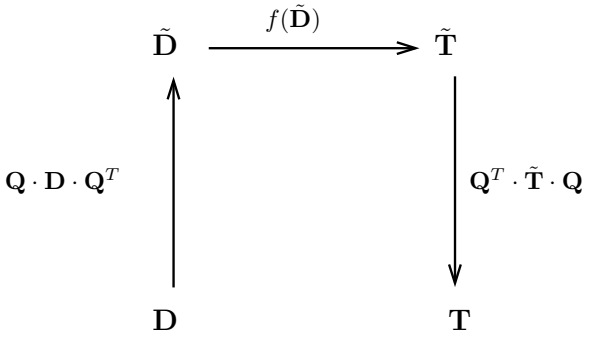


Figure 1: Transformation diagram ($\mathbf{Q}$ is the transformation matrix, in this case a pure rotation tensor.)

and elongation strain rates:

$$\begin{aligned}\tilde{\mathbf{T}}^* &= 2\eta_{\dot{\gamma}}\left(\dot{\gamma}^*\right)\tilde{\mathbf{D}}^*\,,\\ \tilde{\mathbf{T}}^+ &= 2\eta_{\dot{\epsilon}}\left(\dot{\epsilon}^+\right)\tilde{\mathbf{D}}^+\,.\end{aligned} \tag{13}$$

Eventually the resulting two stress tensors, one for shear, one for elongation, have to be combined to a final stress tensor using a proper weighting function.
The third method represents a fully tensor approach, where each component of the shear- and elongation strain tensor is separately taken for the stress tensor component calculation, it reads:

$$\begin{aligned}\tilde{\mathbf{T}}^*_{ij} &= \eta_{\dot{\gamma},ij}\left(\tilde{\mathbf{D}}^*_{ij}\right)\tilde{\mathbf{D}}^*_{ij}\,,\quad i\neq j\,,\\ \tilde{\mathbf{T}}^+_{ii} &= \eta_{\dot{\epsilon},ii}\left(\tilde{\mathbf{D}}^+_{ii}\right)\tilde{\mathbf{D}}^+_{ii}\,,\end{aligned} \tag{14}$$

Although the numerical calculation effort is a bit higher, this approach is targeted in this work to demonstrate the capability of the triple tensor decomposition explained in the next chapter.
After calculation of the stresses by applying specific fluid property models, the third step is to transform the stress tensors back into the original global coordinate system:

$$\mathbf{T} = \mathbf{Q}^T\cdot\tilde{\mathbf{T}}\cdot\mathbf{Q}\,. \tag{15}$$

The associated transformation diagram is depicted in Figure 1.
Since in principle the transformation has to be done for shear and elongation separately, because they normally exhibit different principal axes, the resulting tensors have to be combined to one final stress tensor before this stress information can be put into the momentum equation. The stress tensor reads:

$$\mathbf{T} = \omega\cdot\left(2\eta_{\dot{\gamma}}\left(\dot{\gamma}^*\right)\left(\mathbf{D}^*\right)\right)^t + (1-\omega)\cdot\left(2\eta_{\dot{\epsilon}}\left(\dot{\epsilon}^+\right)\mathbf{D}^+\right)^t\,, \tag{16}$$

when equtaion (13) is used, and:

$$\mathbf{T}_{lm} = \omega\cdot\left(2\eta_{\dot{\gamma},ij}\left(\tilde{\mathbf{D}}^*_{ij}\right)\tilde{\mathbf{D}}^*_{ij}\right)^t_{lm} + (1-\omega)\cdot\left(2\eta_{\dot{\epsilon},ii}\left(\tilde{\mathbf{D}}^+_{ii}\right)\mathbf{D}^+_{ii}\right)^t_{lm}\,, \tag{17}$$

in case of equation (14). In these equations *t* marks the back-transformation, whereas $\omega$ is a weighting function, which has to be defined.

## 3 The Extended Optimal Triple Tensor Decomposition

A suitable transformation tensor Q is still missing. Thereto, in this work a novel approach is presented: it is based on the triple decomposition of the velocity gradient tensor in a pure rotational part, a pure shearing part and a simple shear, respectively a non-rotating elongational, part

following the triple decomposition method (TDM) of Kolář [13]. This method was originally developed to identify vortices in complicated vortical related flows. A proper re-orientation of a basic reference coordinate system allows to distinguish rotational, an effective shear and, finally, the elongational motions. Kolář introduces the new basic reference system by applying iteratively rotation-tensor operations to the original coordinate system, until a shear tensor of maximal effective shear can be decomposed. The components of the associated rotation tensor $\mathbf{Q}$ are determined by the following maximization:

$$\begin{aligned} &\left(\|\mathbf{D}_{12}\mathbf{\Omega}_{12}\| + \|\mathbf{D}_{23}\mathbf{\Omega}_{23}\| + \|\mathbf{D}_{31}\mathbf{\Omega}_{31}\|\right)^{BRF} = \\ &max\left(\|\mathbf{D}_{12}\mathbf{\Omega}_{12}\| + \|\mathbf{D}_{23}\mathbf{\Omega}_{23}\| + \|\mathbf{D}_{31}\mathbf{\Omega}_{31}\|\right)^{all} . \end{aligned} \tag{18}$$

Which algorithm is the best to determine the final rotation tensor $\mathbf{Q}$ is point of discussion and further hints to the geometrical interpretation can be found in [14]. After applying this iterative algorithm the resulting rotating tensor $\mathbf{Q}$ can be used to transform the velocity gradient tensor, see Figure 1, into the new reference frame, which is called *Basic Reference Frame*:

$$grad\ \vec{v}|^{BRF} = \mathbf{Q}\ grad\ \vec{v}|^{xyz}\ \mathbf{Q}^T . \tag{19}$$

Then the components of the transformed velocity gradient tensor are used to calculate the so-called residual tensor $\mathbf{RES}|^{BRF}$:

$$\mathbf{RES}|^{BRF} = \begin{pmatrix} \frac{\partial u}{\partial x} & (sign\frac{\partial u}{\partial y})MIN(|\frac{\partial u}{\partial y}|,|\frac{\partial v}{\partial x}|) & (sign\frac{\partial u}{\partial z})MIN(|\frac{\partial u}{\partial z}|,|\frac{\partial w}{\partial x}|) \\ (sign\frac{\partial x}{\partial x})MIN(|\frac{\partial u}{\partial y}|,|\frac{\partial v}{\partial x}|) & \frac{\partial v}{\partial y} & (sign\frac{\partial v}{\partial z})MIN(|\frac{\partial v}{\partial z}|,|\frac{\partial w}{\partial y}|) \\ (sign\frac{\partial w}{\partial x})MIN(|\frac{\partial u}{\partial z}|,|\frac{\partial w}{\partial x}|) & (sign\frac{\partial w}{\partial y})MIN(|\frac{\partial v}{\partial z}|,|\frac{\partial w}{\partial y}|) & \frac{\partial w}{\partial z} \end{pmatrix} . \tag{20}$$

From the residual tensor a new tensor $grad\vec{v}_{SH}|^{BRF}$, containing only shear-rate related components (also possibly rotated), can be split off:

$$grad\ \vec{v}_{SH}|^{BRF} = grad\ \vec{v}|^{BRF} - \mathbf{RES}|^{BRF} . \tag{21}$$

The residual tensor can be further decomposed into a pure-rotation tensor and a strain tensor, in which only non-rotation related elongational, respectively extensional, rate of strain components occur:

$$\mathbf{RES}|^{BRF} = \frac{1}{2}\left[\mathbf{RES}|^{BRF} - \mathbf{RES}^T|^{BRF}\right] + \frac{1}{2}\left[\mathbf{RES}|^{BRF} + \mathbf{RES}^T|^{BRF}\right] . \tag{22}$$

This can be rewritten to:

$$\mathbf{RES}|^{BRF} = \mathbf{\Omega}_{vortex}|^{BRF} + \mathbf{D}_{EL}|^{BRF} , \tag{23}$$

a formulation which Kolář utilized for the identification of vortices.
In this context focal points of the tensor based fluid modeling are the non-rotating elongation rate tensor $\mathbf{D}_{EL}|^{BRF}$ and the tensor $grad\ \vec{v}_{SH}|^{BRF}$ containing the effective shear rates. Now, the first tensor can be used to calculate the elongation stresses directly. The latter tensor $grad\ \vec{v}_{SH}|^{BRF}$ still contains rotational parts within its strain rates components, thus, in a further step a Chauchy-Stokes decomposition is performed leading to an asymmetric rate of rotation tensor $\mathbf{\Omega}_{SH}|^{BRF}$ and a symmetric rate of "shear" tensor $\mathbf{D}_{SH}|^{BRF}$:

$$grad\ \vec{v}_{SH}|^{BRF} = \mathbf{\Omega}_{SH}|^{BRF} + \mathbf{D}_{SH}|^{BRF} . \tag{24}$$

Now, both tensors, $\mathbf{D}_{SH}|^{BRF}$ and $\mathbf{D}_{EL}|^{BRF}$, are available to feed the specific non-Newtonian fluid models for the application case, and the associated shear and elongation rates, $\dot{\gamma}_{SH}$ and

$\dot{\epsilon}_{EL}$ can be calculated as input for equation (13) or (14), depending on the model approach chosen, before applying equation (16) respectively (17). In this work the latter approach has been implemented which means that each tensor component contributes independently to the momentum equation in the $div\ \mathbf{T}$ term.
It has to be remarked that the proposed approach delivers only an approximate model, because only one reference frame, in which the shear viscosity dominates, is calculated, since it assumes that the elongational motion has roughly the same principal axes of straining. Furthermore, it is not valid for rotating reference systems. In those cases extensions have to be developed, i.e. following the considerations of Wedgewood [27], which lead to formulations of co- and contravariant Oldroyd derivatives and the need for further transport equations. Nevertheless, further research work is needed.

## 4 The Non-Newtonian Fluid Model and the Simulation Setup

Now, the specific non-Newtonian fluid property models have to be introduced to bridge the gap between the strain and stress on the specific fluid material level. Then the flow configuration and simulation setup will be explained.

### 4.1 Properties of the Non-Newtonian Carreau Fluid

As mentioned above, in this study a specific class of non-Newtonian fluids are considered: the shear-thickening and elongational-thinning fluids without any yield stress or temporal relaxation properties. Also the impact of temperature on the viscosity is neglected. When calculating the fluid viscosity properties, then, instead of targeting for a generalized shear rate, $\dot{\gamma} = \sqrt{\frac{1}{2}\left[\mathbf{D} : \mathbf{D}\right]}$, which is commonly taken as input into a generalized Newtonian fluid model, the reduced shear rate $\dot{\gamma}_{SH}$, reflecting the simple shear flow motion, and the elongation rate $\dot{\epsilon}_{EL}$, representing the elongational fluid motion, have to be determined[2]. Then for both different strain rates a specific viscosity models can be applied. For covering the shear-thickening viscosity effect the fluid model of Wei et al. [28] was adapted and applied:

$$\eta_{\dot{\gamma}}\left(\dot{\gamma}\right) = \eta_{\dot{\gamma},0} + \eta_{\dot{\gamma},max}\left(1 - \frac{1}{1 + exp(k_1\dot{\gamma} + w_1)}\right)\left(\frac{1}{1 + exp(k_2\dot{\gamma} + w_2)}\right). \tag{25}$$

In this equation $n_{\dot{\gamma},0}$ and $n_{\dot{\gamma},max}$ are the zero-Newtonian and the maximal possible viscosity, $k_1$, $k_2$, $w_1$ and $w_2$ are further flow curve parameters to be adjusted to fit experimental viscosity measurement results.
For covering the elongation-rate caused viscosity thinning effect, the Carreau fluid model [6] has been applied, which possesses both a constant zero-Newtonian viscosity and a constant infinite-Newtonian viscosity, also called upper- and lower-Newtonian viscosity plateaus. These viscosity limitations are reflecting the properties of real fluids very well [2]. It also exhibits the log-law behaviour of the viscosity change under shearing or elongational flows. It further features parameter-controlled smooth transitions between viscosity log regions and the Newtonian plateaus. This model is often used for polymer melts [3], but also for extensional flows [21]. The flow curve of a Carreau fluid reads

$$\eta_{\dot{\epsilon}}\left(\dot{\epsilon}\right) = \eta_{\dot{\epsilon},0} + \frac{\eta_{\dot{\epsilon},0} - \eta_{\dot{\epsilon},\infty}}{\left(1 + \left(\lambda_{\dot{\epsilon}}\dot{\epsilon}\right)^2\right)^{\frac{(1-n_{\dot{\epsilon}})}{2}}}, \tag{26}$$

[2] In the following the indices SH and EL are omitted.

in which $n_{\dot{\epsilon}}$ is the power-law index, $\eta_{\dot{\epsilon},0}$ the lower Newtonian limit or zero viscosity, $\eta_{\dot{\epsilon},\infty}$ the upper Newtonian limit or infinite viscosity and $\dot{\epsilon}$ the elongation rate[3]. The parameter $\lambda_{\dot{\epsilon}}$ controls the transition from the Newtonian to the non-Newtonian behaviour. This parameter can be determined by the characteristic stress $\tau_\epsilon$, at which the deformation behaviour of the fluid changes: $\lambda_{\dot{\epsilon}} = \eta_{\dot{\epsilon},0}/\tau_{\dot{\epsilon}}$. In principle this time constant is the reciprocal value of the critical elongation rate $\dot{\epsilon}_c$, at which exceeding shear rates start to reduce the viscosity of the fluid. In this simulation study the following fluid parameters are used: the shear thickening flow curve is defined by the following parameter values: $\eta_{\dot{\gamma},0} = 3.461Pas$, $\eta_{\dot{\gamma},max} = 11.609Pas$, $k_1 = 0.277\ s$, $k_2 = 0.068\ s$, $w_1 = -4.037$ and $w_2 = -2.846$, which are describing the fluid properties of suspensions of hydrophobic fumed SiO2 nanoparticles R972 in PPG and the mass of SiO2 of 10%, see [28]. For the elongational thinning fluid the parameters are $n_{\dot{\epsilon}} = 0.2$, $\lambda_{\dot{\epsilon}} = 0.1s$, $\eta_{\dot{\epsilon},0} = 10.383Pas$, $\eta_{\dot{\epsilon},\infty} = 0.004Pas$. Latter values are estimates for this suspension because for this fluid exact data are missing. The associated flow curves are depicted in Figure 2. The small values of the time constant and the power-law index $n_{\dot{\epsilon}}$ are chosen in order to achieve a high sensitivity of the fluid viscosity in particular to lower elongation rates, so that the viscosity can drop orders of magnitudes over the full range of the expected flow elongation rates. This is not non-physical, since low-density polymers, carbon and silicone oils or especially synthesised engine oils reveal such fluid properties. The final stress tensor equation to be used in the

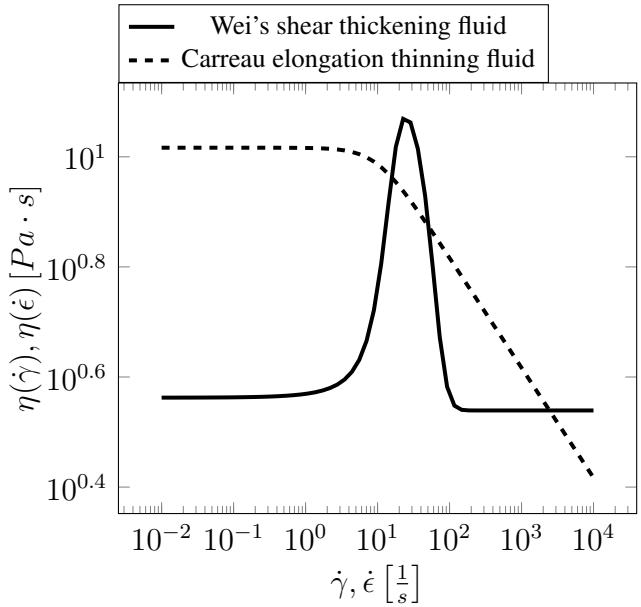


Figure 2: Flow curve for a shear thicking fluid model of Wei [28], the second flow curve (dashed) represents an elongational thinning Carreau fluid [6].

application case combines the stress tensor parts according to equation (17) by introducing a weighting function:

$$\omega = \begin{cases} \frac{\dot{\gamma}}{\dot{\gamma}+\dot{\epsilon}}\,, & \dot{\gamma}+\dot{\epsilon} > 10^{-5} \\ 1\,, & else \end{cases} \tag{27}$$

This weight assumption is chosen to reflect an evenly valued effect of shear or elongation on the viscosity; of course, validated weighting functions have to be determined experimentally in order to accurately fit the viscous fluid properties.

[3]In the following the index $\dot{\gamma}$ indicates shear, $\dot{\epsilon}$ refers to elongation.

### 4.2 Flow Configuration and CFD Setup

A cross-slot channel flow configuration, consisting of four perpendicularly orientated crossing channels, has been selected as technical application, since due to its geometrically flow-constraining walls strong elongational effects, stretching or compression, are expected at the channel intersection region [19]. It is well known that viscoelastic effects can be well investigated in such a flow configuration [26], [8], however, even for non-elastic viscous fluid flows this flow configuration shall reveal significant effects on the viscosity properties of a shear and elongational sensitive fluid. Inspired by Schoonen's cross-slot design a custom configuration was derived, a CAD geometry was drawn and a CFD grid generated. The corresponding 2D configuration is depicted in Figure 3. Each channel of the cross-slot configuration has a width

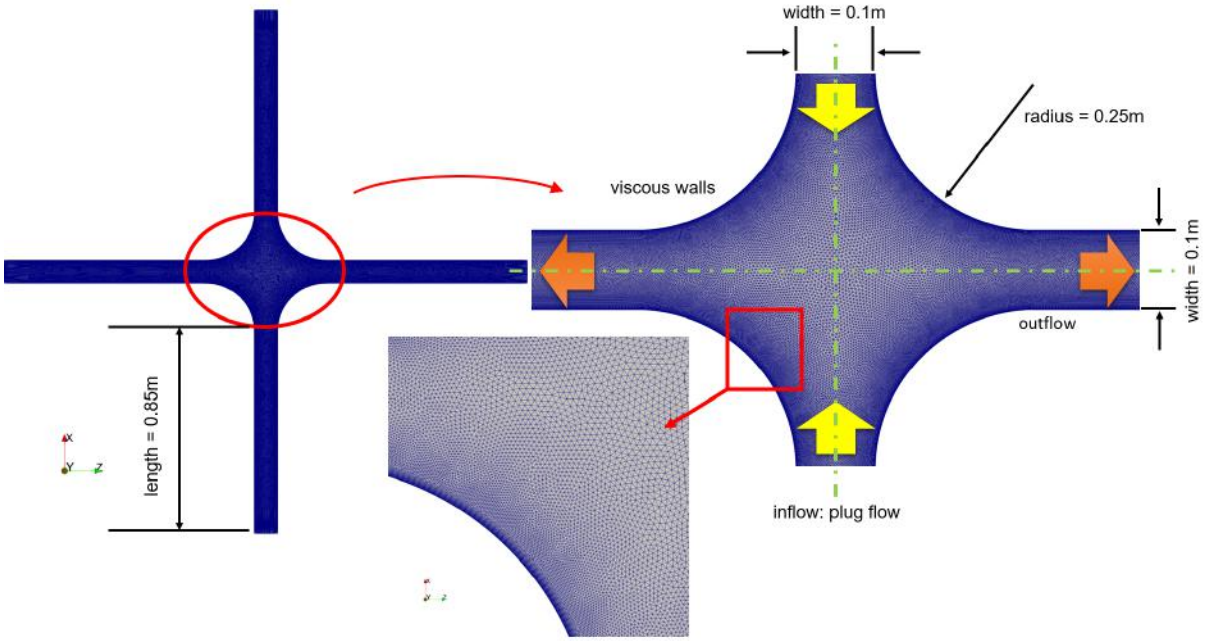


Figure 3: CFD configuration, grid details and basic numerical setup.

of $0.1\mathrm{m}$ and possesses a straight section of $0.85\mathrm{m}$ before the quarter-circled crossing section follows. The radii of the quarter circles are $0.25\mathrm{m}$ each. The associated CFD grid has been generated with the mesh generator Centaur from CentaurSoft [7]. The resulting relatively small, partially structured and unstructured 2D hybrid CFD grid consists of approximately 148000 vertices. They are ordered in nearly 53000 quadratic cells in 30 structured layers, especially layered for resolving the boundary layer flow. The first grid cell height of the structured layer is 0.002 mm and with an increasing distance to the wall the prismatic cell heights are growing with a growth rate of 1.2. Round about 189000 triangles filling up the inner flow field space. The CFD simulations have been performed using the DLR flow solver THETA wich is a spin-off of the DLR TAU code [9]. This second order edge-based finite-volume code solves the incompressible Navier-Stokes equations. For the calculation of the steady, laminar flow field, the quadratic upwind differencing scheme (QUDS), a multigrid acceleration techniques (V3) and a velocity-pressure coupling method (SIMPLE) have been applied. At the top and bottom channel entries a plug flow with an intruding velocity of $0.5\ m/s$ has been prescribed. The low speed, the high density of the fluid of $1007\ kg/m^3$ and the initial zero-Newtonian viscosity of the applied fluid model of $3.461\ Pas$ guarantee a laminar, in fact, creeping flow with a very low Reynolds number of $14.5$. The self adjusting exit-pressure boundary condition has been used at the far left and right outflow panels, all other panels have been treated as viscous walls.

For comparison, a second fluid material model has been considered for the same flow configuration. Here, a pure shear thickening Carreau fluid flowing through the cross slot channels. The first Newtonian plateau is set to $3.461Pas$, the power-law index was set to $n = 1.2$ and $\lambda = 0.1$. Other parameters, for example the second Newtonian plateau value, do not play a role. It has to be remarked that such a comparison has only a limited expressive power, since significant features of the original fluid can not be represented. Nevertheless, the objective is to demonstrate that tensor based fluid model approaches have a rationale for their existence. Of course, experimental validation would be desirable, however, flow field measurements are complicated and often barely possible, in particular for fluid material blends, which prevent optical access i.e. for particle image velocimetry due to changes of their material transparency. Hence, experimental validation data are missing and new measurement techniques are urgently needed.

## 5 Analysis and Discussion of Simulation Results

Now, the results of the simulation study are analysed. Hereto, in the following only a magnified cutout of the cross-slot central part is considered, since the pure channel flows do not exhibit any special features. In the following figures both numerical flow simulation results are compared side by side, each on the left the outcome with the fluid featuring only the shear thickening behaviour, and each on the right the fluid exhibiting shear thickening and elongational thinning behaviour, as explained in the previous chapter. It has to be remarked that besides the velocity field the comparison of the field data are based on derived quantities which are not directly used in the stress tensor calculation for the momentum equation: The shear and elongation rates are outcome of classical strain rate calculations of the corresponding rate of deformation tensors, the effective vicosity is calculated following (12). Currently techniques for full tensor-based comparisons are topic of further research. The disadvantage to be acceppted is that flow structures might to be exaggerated.

To get a first impression of the flow fields, the velocity field is visualised using the Line

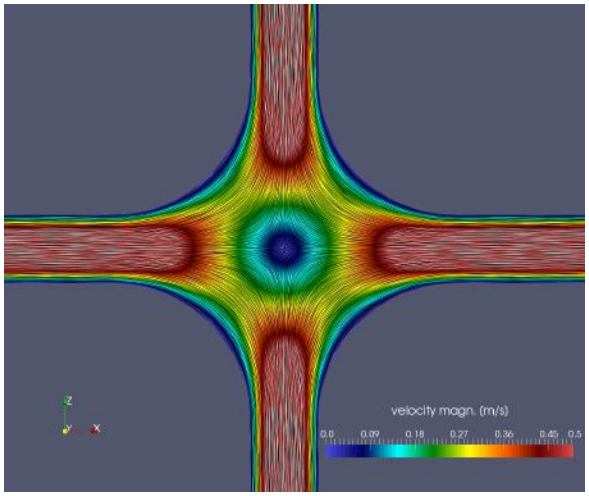


a) Only shear thickening flow case using Wei's fluid model [28].

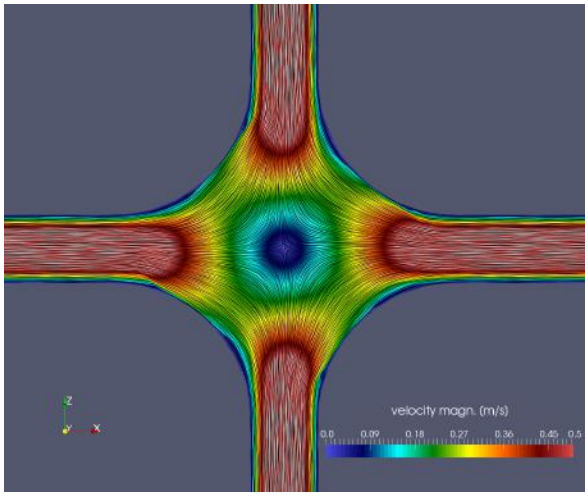


b) Wei's shear thickening and elongational thinning Carreau fluid flow case.

Figure 4: LIC visualisation of the velocity field colour coded by its magnitude.

Integral Convolution technique (LIC) for depicting the velocity directional information, which is also colour coded by the velocity magnitude. The left picture of Figure 4 reveals a quite symmetric flow with kinematically compressing, extension and shearing parts, typical for a wall

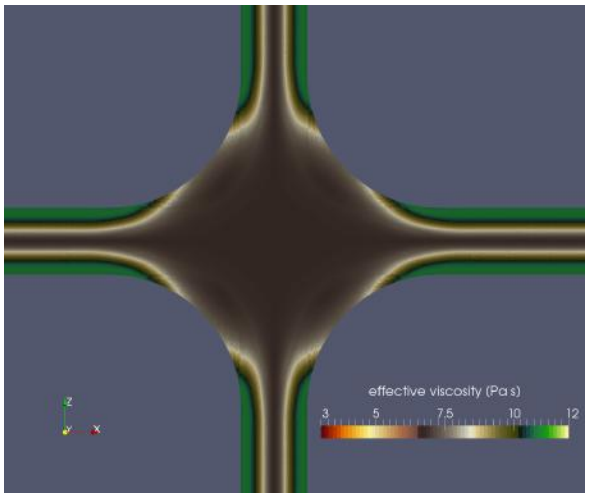


a) Only shear thickening flow case using Wei's fluid model.

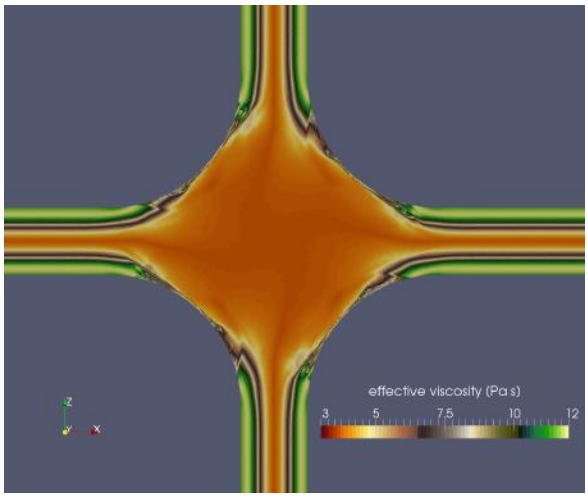


b) Wei's shear thickening and elongational thinning Carreau fluid flow case.

Figure 5: Visualisation of the effective viscosity field according to equation (12).

constrained saddle point flow. On the right, the flow structure exhibits a disturbed symmetry by a slight counter-clockwise rotation of the core region of the flow. This indicates that the elongational thinning has amplified a flow instability so much that it could manifest in the flow field. This amplification is only possible when the elongational zero-Newtonian viscosity of the fluid model is strongly lowered due to elongational loads. As Figure 5 reveals, this, indeed, is the case: in comparison to the effective viscosity depicted on the left side, the image on the right side shows a two times lower effective viscosity. This results in a increased fluidity which allows a flow adaptation against the more strict compressing of the saddle point flow structure. That the elongation flow type significantly dominates the shear flow type in the cross-slot middle section is an intentional result of the configuration design. The shear rates of both flow cases, depicted in the left and right image of Figure 6 is confirming this: the shear rate values are of the same level, carefully compared their values are not quite different, even in the cross-slot core region they are of similar value. That the elongation flow type significantly dominates the shear flow type in the cross-slot middle section is an intentional result of the configuration design. The shear rates of both flow cases, depicted in the left and right images of Figure 6 are confirming it: the shear rate values are of the same level, carefully compared their values are not quite different, even in the cross-slot core region they are of similar value. Therefore, only the elongation rates can have a crucial impact on the viscosity. Since this lowering effect is not present in the pure shear thickening flow case in Figure 7 the elongation rates are shown only for the shear and elongation sensitive fluid flow. In principle, there are two separated regions with high elongation rates: the cross-slot core region with peaks at the channel openings and at the curved side walls. There seems to be an interaction between shear and elongation flow types due to the wall acting as diffusor on the one hand and as a vent on the other hand. The curvature seems not to be optimal for such a flow

As shown, the slightly redirected flow stream leads to flow separation at the curved walls, and, obviously, some overshootings in the effective viscosity, the shear and elongation rate distributions are visible. The sharp kinks point out some further instabilities of numerical or flow physical kind, perhaps exxagerated by the visualised quantities. Unfortunately, experimental data are missing for further validation purposes and discussion of expected flow phenomena. Nevertheless, these CFD results, which have been presented, are beneficial, because it could be demonstrated that a tensor based approach for fluid viscosity modeling can help to reveal fluid

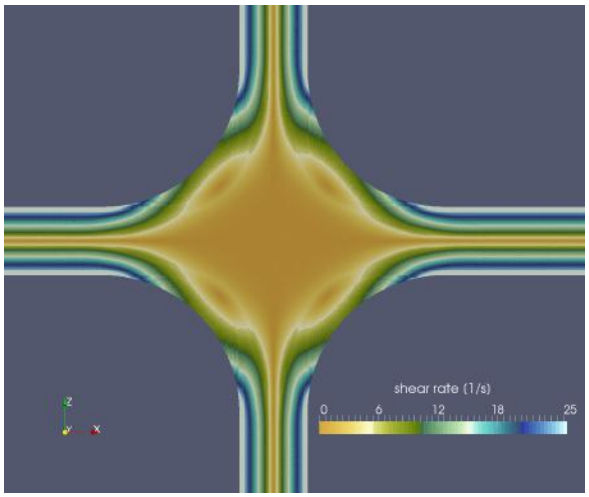


a) Only shear thickening flow case using Wei's fluid model.

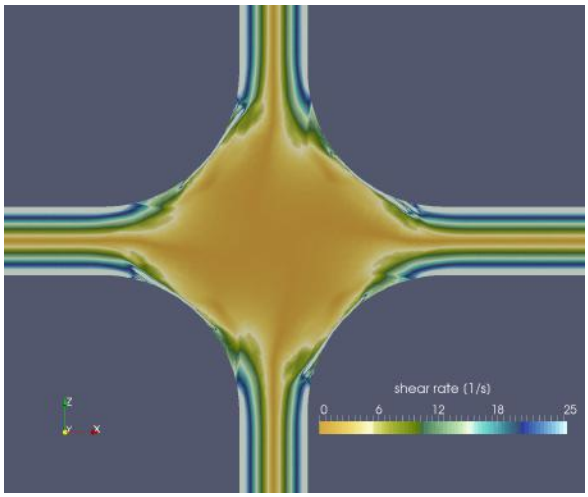


b) Wei's shear thickening and elongational thinning Carreau fluid flow case.

Figure 6: Visualisation of the shear rate field $\dot{\gamma}_{SH}$.

and flow related viscosity properties which are strongly depending on the underlying flow type.

## 6 Conclusion

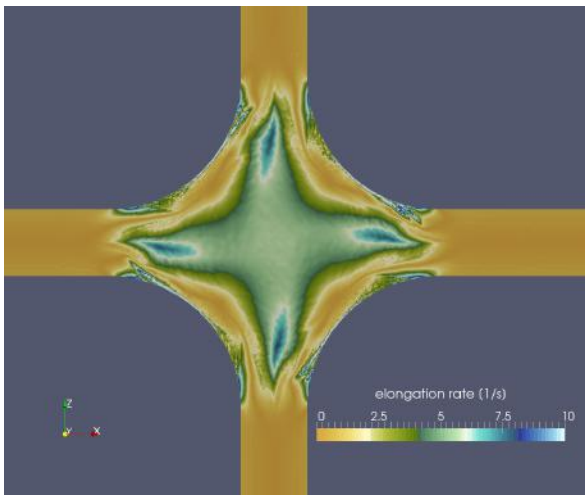


Figure 7: Visualisation of the elongation rate field $\dot{\epsilon}_{EL}$.

In this work a novel tensor based fluid model for the prediction of non-Newtonian shear and elongation thickening and thinning viscosities is introduced, taking into account kinematically different flow types. The special problem of the distinction of shearing and elongational flows has been explained in detail. It is obvious, that this can lead to an inadequate modeling of fluid properties, moreover, it can even prevent the detection of significant flow phenomena. Hence, more advanced tensor based model approaches are necessary. Therefore, the optimal triple tensor decomposition, originally developed in the framework of vortex dynamics, was extended and adapted to the special needs of non-Newtonian fluid model representation. It was demonstrated that this tensor approach allows to determine distinct strain rate information which can be utilised in well-known fluid models, i.e. GNF model variations. With the performed CFD study it could be further demonstrated, by investigating the non-Newtonian cross-slot channel flow, that the presented optimal triple tensor decomposition based approach has its own rationale for existence due to the fact that it reveals the high sensitivity of the designed fluid to elongational thinning viscosity. It is assumed that the physical mechanism behind the observed flow phenomenon, the breaking of the flow symmetry, is an amplification of flow instabilities. Latter should be a focal point for further investigations in particular by conducting flow field measurements in validation experiments. The introduced optimal triple tensor

decomposition has the potential of additional extension to other fluid models, i.e. viscoelastic fluid models could also be formulated in order to distinguish between shear and elongation oscillating behaviour revealing novel flow phenomena in particular in polymer melts.

**Acknowledgment**

The author would like to thank the German Aerospace Center (DLR) and the University of Kassel for greatly supporting this research work.

**REFERENCES**

[1] Astarita, G. and Marrucci, G.: Principles of non-Newtonian fluid mechanics. McGraw-Hill Book Company (UK) Limited, London, New York, 1974

[2] Bird, R. B.: Non-Newtonian behavior of polymeric liquids. Physica A: Statistical and Theoretical Physics, Vol. 118, No. 1–3, pp. 3-16, 1983

[3] Bird, R. B., Hassager, O.: Dynamics of Polymeric Liquids: Vol.1: Fluid Mechanics. Series: Dynamics of Polymeric Liquids, London, New York, John Wiley & Sons, 1987

[4] Bobyarchick, A.; The Eigenvalues of Steady Flows in Mohr Space, Tectonophysics, Vol. 122, pp. 35–51, 1986

[5] Böhme, G.: Strömungsmechanik nichtnewtonscher Fluide. ISBN 9783519123545, Leitfäden der angewandten Mathematik und Mechanik, Teubner, 2000

[6] Carreau, P. J.: Rheological equations from molecular network theories. J. Rheol., Vol. 16, No. 1, pp. 99-127, 1972.

[7] www.centaursoft.com

[8] Coventry, K. D. and Mackley, M. R.: Cross-slot extensional flow birefringence observations of polymer melts using a multi-pass rheometer, J. of Rheology, Vol. 52 (2), pp. 401–415, 2008

[9] Gerhold, T., and Evans, J.: Efficient computation of 3D-flows for complex configurations with the DLR-TAU code using automatic adaptation. New Results in Numerical and Experimental Fluid Mechanics II, 1999.

[10] Haller, G.: A variational theory of hyperbolic Lagrangian coherent structures. Physica D, Vol.240, pp. 574–598, 2011

[11] Han, C. D. and Lamonte, R. R. and Shah, Y. T.: Studies on melt spinning. III. Flow instabilities in melt spinning: Melt fracture and draw resonance. J. Appl. Polymer Sci., Vol. 16, pp. 3307–3323, 1972

[12] Hill, C. A. and Cuculo, J. A.: Elongational Flow Behavior of Polymeric. J. of Macromolecular Science, Vol. 14(1), pp. 107–153, 1976

[13] Kolář, V.: Vortex identification: New requirements and limitations, International J. of Heat and Fluid Flow, Vol. 28, pp. 638–652, 2007

[14] Kolář, V., Šístek, J., Fehmi Cirak, F. and Moses, P.: Average Corotation of Line Segments Near a Point and Vortex Identification, AIAA JOURNAL, Vol. 51, No.11, 2013

[15] Lamonte, R. R. and Han, C. D.: Studies on Melt Spinning. II. Analysis of the Deformation and Heat Transfer Processes. J. Appl Polymer Sci., Vol. 16, pp. 3285 – 3306, 1972

[16] Laun, H. M. and Münstedt, M.: Elongational behaviour of a low density polyethylene melt. Rheol. Acta, Vol. 17, pp. 415–425, 1978

[17] Means, W. D.: Application of the Mohr-circle construction to problems of inhomoheneous deformation. J. Struct. Geol., Vol. 5. pp. 279–286, 1983

[18] Peacock, Th. and Haller, G.: Lagrangian coherent structures. The hidden skeleton of fluid flows, Physics Today, Vol. 66, No. 2, pp. 41–47, 2013

[19] Peters, G. W. M., Schoonen, J. F. M., Baaijens, F. P. T. and Meijer, H. E. H.: On the performance of enhanced constitutive models for polymer melts in a cross-slot flow. J. of Non-Newtonian Fluid Mech., 82(2-3), pp. 387–427, 1999

[20] Petrie, C. J. S: Elongational Flows. Research Notes in Mathematics Series, Pittman Publishing, London, ISBN 9780273084068, 1979

[21] Petrie, C. J. S.: Extensional flows. Rheology Series, Vol. 8, pp. 613–636, 1999

[22] Petrie, C. J. S.: One hundred years of extensional flow. J. Non-Newtonian Fluid Mech., Vol. 254, pp. 1–14, 2006

[23] Petrie, C. J. S.: Extensional viscosity: a critical discussion, J. Non-Newtonian Fluid Mech., Vol. 254, pp. 15–23, 2006

[24] Reyn, W. J.: Classification and Description of the Singular Points of a System of Three Linear Differential Equations. ZAMM J. of Applied Mathematics and Mechanics / Zeitschrift für Angewandte Mathematik und Mechanik, Vol. 15, pp. 540–557, 1964

[25] Rubart, L. and Böhme, G.: Numerical Simulation of Shear-Thinning Flow problems in Mixing Vessels. Theoretical and Computational Fluid Mechanics, Vol. 3, pp. 95–115, 1991

[26] Schoonen J. F. M., Swartjes, F, H. M., Peters, G. W.M., Baaijens, F. P. T. and Meijer, H. E. H.: A 3D numerical/experimental study on a stagnation flow of a polyisobutylene solution. Dedicated to Professor Marcel J. Crochet on the occasion of his 60th birthday.1, J. of Non-Newtonian Fluid Mech., Vol. 79, Issues 23, pp. 529–561, 1998,

[27] Wedgewood, L.: An objective rotation tensor applied to non-Newtonian fluid mechanics. Rheol. Acta, Vol. 38, pp. 91–99, 1999

[28] Wei, M., Sun, L., Qi, P., Chang, C. and Zhu, C.: Continuous phenomenological modeling for the viscosity of shear thickening fluids, J. Nanomaterials and Nanotechnology, Vol. 8, pp. 1–7, 2018

[29] Yao, Donggang: A non-Newtonian fluid model with an objective vorticity. J. of Non-Newtonian Fluid Mech., Vol. 218, pp. 99-105, 2015